Hemodynamics inside a human left coronary artery

E. Jabir, S. Anil Lal
Department of Mechanical Engineering
College of Engineering, Trivandrum
e_jabir@yahoo.com
anillal@cet.ac.in

***Abstract*—Diseases affecting cardio-vascular system continues to be a major cause of death in modern world. Atherosclerosis caused by the accumulation of fatty material such as cholesterol inside the inner layer of artery walls is a very common example. The biological stimuli for this disease is diffuse throughout entire artery tree, but in practice atherosclerosis is found to be very focal and localises at some areas like bends and bifurcations of high pressure arteries. It has been proven in the literature that, fluid dynamical properties of blood such as wall shear stress (WSS) and vorticity variations play vital role in the localisation of atherosclerosis. Locations with lower value of WSS is found to be more prone to the fat plaque depositions. In the present work, tools of computational fluid dynamics (CFD) are applied to understand flow physics in a realistic model of Left coronary artery (LCA) with physiologically accurate pulsatile boundary conditions. Geometric model of LCA is extracted from a high resolution computed tomography (CT) dataset using an image segmentation method. The unsteady flow rate through the LCA measured using Doppler ultrasound method, reported in the literature are served as boundary conditions for the analysis. Large eddy simulation (LES) is used to resolve turbulent features of flow. A framework fully based on available open source software is developed and used. The variation of wall shear stress and the distributions of velocity and vorticity in accordance with the inlet pulse is studied and presented.**

Keywords*—Cardio-vascular fluid mechanics, atherosclerosis, patient specific modelling, image segmentation.

I. Introduction

Blood flow inside the cardio vascular system is a transient phenomenon driven by the cyclic expansion and contraction of heart. The velocity field is assumed to have a periodic pulsatile behaviour, varying between zero when the tricuspid aortic valve is closed, and a maximum during the systole ([1], [2]). Blood flow is believed to be of laminar nature in most situations, but the branches, curves and other asymmetries present in the vascular system can bring three dimensional flow features such as complex vortical structures, flow separations and recirculation zones [3] to the flow field. These 3D features significantly alters the local hemodynamic parameters and play a vital role in the development of decease like atherosclerosis, which is caused by the accumulation cholesterol within the arterial wall [4]. Atherscherosis may results in local constriction of the vessel called stenosis and can inhibit the blood supply of downstream tissues. In practice, it is found that stenosis develops preferentially in regions of low shear stress on the artery wall. It is widely accepted that there is a strong relationship between complex velocity patterns and shear stress distributions with the location of atherosclerosis [5], [6]. Sudden rupture of atherosclerotic plaque inside an artery may result in the creation of a thrombosis which partially or completely stops the blood flow. Downstream tissues may suffer ischemic changes leading to their permanent death. Most common example of this situation is the myocardial infarction commonly known as heart attack caused by the atherosclerosis in coronary arteries.

The left coronary artery (LCA), which feeds blood to the left side of the myocardium originates from the aortic root and in most of the cases gets bifurcated to left anterior descending artery (LAD) and left circumflex artery (LCX). In general, coronary arteries are found very predisposed to atherosclerosis and stenosis due to their peculiar branching patterns and high oscillating pressure gradients. Observations based on 300 autopsies presented by Enos et.al. [7] disclosed the constant pattern in the location of plaque depositions. It is reported that at the bifurcation, plaques are constantly found on the wall of LCA opposite to the ostium of the LCX. Their study also revealed that localisation of atherosclerosis is apparent in proximal arteries and their branches compared to the distal regions. In a similar work, Grøttum et.al [8] clinically studied the detailed distribution of atherosclerotic lesions in the branching region of LCA. The distinct spatial distribution patterns of atherosclerotic lesions were identified to have a high frequency of occurrence on the outer walls and at the inner curvature of the bifurcation at the downstream side.

Experimental investigations of vascular dynamics and flow are very complicated due to small sizes and the complexity of vessel structure. Therefore, theoretical-mathematical models and computer simulations have particular importance. Flow of blood through arteries can be mathematically modelled by the fundamental equations of fluid dynamics. The techniques of computational fluid dynamics (CFD) can be used to solve these equations numerically and to study the flow physics in the presence of atherosclerosis plaque formations which can forecast further development of the decease. In the current scientific literature several researchers are working on numerical simulations of blood flows in coronary arteries under different conditions. Perktold et.al. [9] studied the pulsatile flow field in an anatomically realistic model of LAD first diagonal bifurcation numerically and compared with laser Doppler anemometry measurements. Physiologically realistic inlet velocity profiles and geometric model were used in the computer simulation. The comparison of computed and measured axial velocity results showed good agreement. A detailed three dimensional study using an idealistic LCA model with approximate dimensions extracted from angiographies is reported in [10]. Distribution of wall shear stress (WSS) over the entire normal human LCA tree was presented. As expected the low WSS regions occurred in bifurcations oppo-

site to the flow dividers which are identified as anatomic sites predisposed for the development of atherosclerosis. Although most of the studies conducted in the past are based on idealistic geometries, in the last few years researchers started to use realistic anatomies, extracted from computed tomography (CT) or Magnetic resonance imaging (MRI) datasets. The geometric model reconstructed from these scan datasets is a pre-requisite for obtaining accurate and reliable results from CFD simulations. In a recent work Chaichana et.al [11] conducted a comparison between the hemodynamic predictions obtained using idealistic and realistic geometric models of LCA. Distribution of WSS and its gradient with different bifurcation angles are presented. Their findings pointed out the existence of a strong relationship between the wide angulation of the LCA bifurcation and WSS. Habib et.al. [12] conducted computational simulations in coronary arteries and compared WSS distributions with experimentally measured values over time using intravascular ultrasound scanning method. Subject specific geometric data and boundary conditions are used for the analysis. They concluded that while low WSS bearing artery segments suffer constrictive remodelling, high WSS segments develop excessive expansive remodelling.

The present work is targeted to numerically simulate and study the flow physics in left coronary artery using computational fluid dynamics. Geometric data obtained form a high resolution CT dataset together with pulsatile inlet conditions already reported in the literature are used. An open-source CFD package OpenFOAM [13], based on the finite volume discretisation of the governing equations of fluid motion is used to solve the flow field. Turbulent features of the flow field are resolved using Large eddy simulation (LES) technique and the shear thinning nature of the blood is taken in to account by using Carreau viscosity model. The variation of wall shear stress, distributions of velocity, pressure and vorticity are studied under pulsatile flow conditions and presented.

A. Vascular reconstruction and grid generation

Construction of the geometric model is a prerequisite for the numerical simulation of hemodynamics. The complex vascular structure have to be extracted from a high resolution dataset obtained by MRI image acquisition of the region under consideration. In this work, geometry is obtained from a CT dataset available as part of Rotterdam coronary artery algorithm evaluation framework [14]. Extraction of the vessel lumen from the three dimensional image data is carried out using an open source image segmentation software, Vascular modelling toolkit (VMTK) [15]. VMTK is a framework which can be used for the analysis, visualisation and segmentation of vascular structures. A level set segmentation method with suitable filtering algorithms is used to segment the vessel and after clipping superfluous areas, surface smoothing filters are applied. Main bifurcation of LCA with the first diagonal branch (D1) of LAD is segmented for the present study. Flow extensions having length twice the diameter is added at all sides of the vessel for the application of standard boundary conditions. The resulting surface data is exported to STL (STereoLithography) format for further processing.

The computational grid required for the numerical simulation is constructed using the standard meshing utility included in the OpenFOAM package, snappyHexMesh. It is an advanced

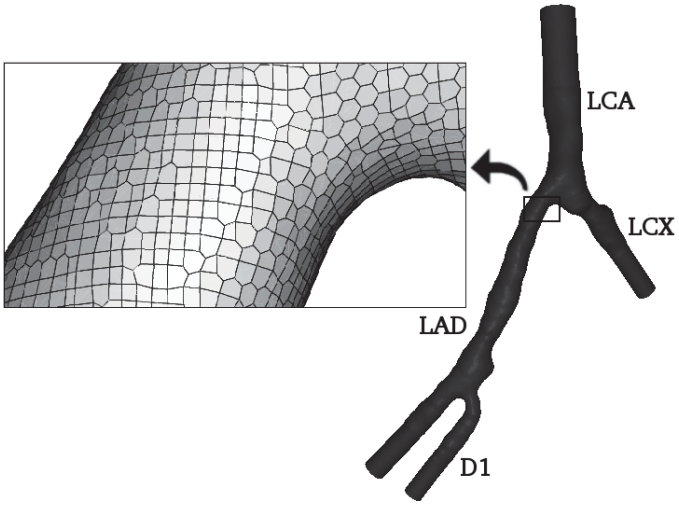

Fig. 1. Segmented LCA surface from CT dataset using VMTK showing LCA trunk, LAD, LCX and the first distal branch (D1) of LAD. An enlarged view of the computational grid generated using snappyHexMesh is shown in the inset.

meshing program having several features for the generation of grids with high quality polyhedral elements and capable of parallel processing. Levels of grid refinement can be set according to specific needs and mesh quality is monitored throughout the meshing process. Fig. 1 shows the vessel surface obtained and the enlarged view of the mesh which has a total of 491842 polyhedral elements. A comparison study conducted with a 25% finer mesh showed a variation less than 5% in the peak value of WSS, proving grid independence.

II. Methedology

A. Fluid and flow properties of blood

Although flow of blood is believed to be laminar in most situations, the branches, curves and other asymmetries present in the vascular system creates three dimensional features in the velocity patterns resulting in complex vortical structures, flow separations and recirculation zones leading to the generation of turbulence [3]. Flow may evolve to fully turbulent or re-laminarise back depending on the intensity of the perturbation induced by these geometric variations. In the present work, LES model is employed to resolve the turbulent features of the flow field. A k-equation eddy-viscosity model is used to filter the subgrid scales.

Blood is assumed as a homogeneous, isotropic and incompressible viscous fluid, with a constant density of $1050\ kg/m^3$. The shear thinning behaviour is modelled using Carreau model [16], which is proven as the best by Johnston et.al [17] to model real blood.

$$\mu_{eff}(\dot{\gamma}) = \mu_{\inf} + (\mu_0 - \mu_{\inf})\left(1 + (\lambda\dot{\gamma})^2\right)^{\frac{n-1}{2}} \quad (1)$$

where μ_0 is viscosity at zero shear rate, $\mu_{\inf}$ is viscosity at infinite shear rate, λ is the relaxation time and n is a power index. These are material coefficients and respective values for human blood are taken from [17] as, $\mu_0 = 0.056\ Pa.s$, $\mu_{\inf} = 0.00345\ Pa.s$, $\lambda = 3.313\ s$ and $n = 0.3568$.

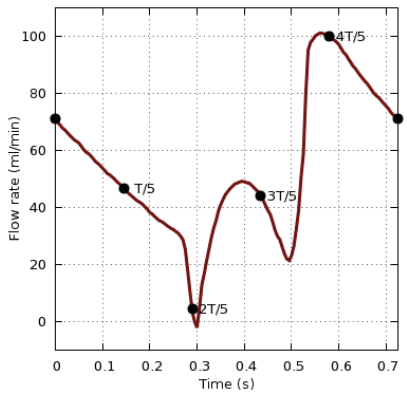

Fig. 2. Pulsatile inflow boundary condition at LCA reported in [1] based on experimental measurements.

B. Boundary conditions

Physiologically accurate pulsating inlet flow rate for LCA shown in Fig. 2 as reported in [1] is used as the inflow boundary condition. The pulse have a time period of 0.725 sec. According to the study of Giessen et.al. [18] based on angiographic measurements, flow splitting ratio through the side branches of an artery bifurcation scales with the ratio of the diameter of the side branches as,

$$\frac{Q_{LAD}}{Q_{LCX}} = \left(\frac{d_{LAD}}{d_{LCX}}\right)^{2.27} \tag{2}$$

where, d and Q denotes the diameters of the daughter branches of bifurcation and corresponding flow rates repectively. For the model considered in the present study, the flow rate division ratio is found to be 0.422 and the calculated outflow rate is imposed at the LCX exit.

While transient inflow and outflow profiles are applied at the LCA and LCX respectively, zero gradient-stress free conditions are imposed at the exit of LAD and D1. No slip boundary condition for velocity and zero normal gradient for pressure are applied on all the walls. Walls of the vessel are considered to be rigid. Absolute pressure at LAD and D1 outlets are taken as zero. Turbulent kinetic energy at the inlet is specified by using the following correlations given by Pope [19],

$$k = \frac{3}{2}\left(V_{avg} \times I\right)^2 \tag{3}$$

where, $I = 0.16(Re)^{-1/8}$, $Re = \frac{\rho V_{avg} D}{\mu}$ is Reynolds number based on the average flow rate over a cycle, ρ is the density and μ is the viscosity.

C. Solution of flow equations

The governing equations of flow field are solved using a PISO algorithm based solver of OpenFOAM package together with a k-equation eddy-viscosity LES model to resolve turbulent scales. Pulsatile flow simulations are conducted for 10 time periods with a sufficiently small time step size of $5e^{-5}$ s, to satisfy the CFL stability criterion. Results are presented for the final time period at five consecutive time intervals

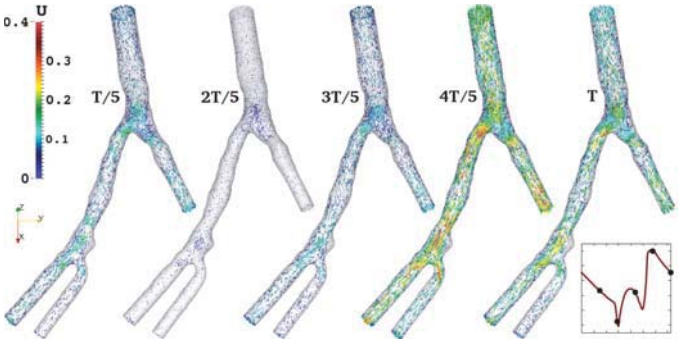

Fig. 3. Velocity vectors in the flow domain at times $T/5, 2T/5, 3T/5, 4T/5$ and T, where T is the period of inlet flow rate pulse.

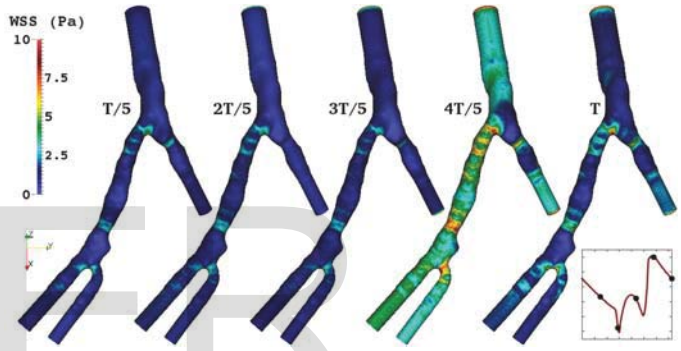

Fig. 5. Spacial distribution of WSS over the LCA surface at different time instances.

and are visualized using an open-source visualization package, ParaView [20].

III. Results and Discussion

The results are presented for five time instances having equal width during one cycle of the inlet pulse. During each cardiac cycle, the inlet pulse reaches its peak systolic velocity around time, $t = 0.4$ s. Spacial distribution of velocity vectors over the flow domain at five consecutive time intervals is shown in Fig. 3 and corresponding stream traces at the first bifurcation are given in Fig. 4. It can be seen that velocity vectors have maximum values at the minimum diameter regions of vessel, like ostium of LAD and the D1 branch. At the deceleration phase, that is for $(0 < t < 2T/5)$ and $(t > 4T/5)$, flow separates from the outer walls of the bifurcation creating recirculation eddies which causes a dramatic reduction in the magnitude of wall shear stress. This behaviour is clearly visible in the streamline plot depicting the formation of a large recirculating vortex at the throat of LCX. When the flow pulse reaches its minimum value, i.e., around $t = 2T/5$, flow rate through LCX also reaches its minimum. In the acceleration phase beyond $T = 3T/5$, as a result of the abrupt change in flow rate, recirculation eddies vanishes suddenly.

Variation of wall shear stress along the artery surface is depicted in Fig. 5. The regions of low WSS are found to be distributed around the bifurcations. As the inlet pulse reaches the peak acceleration, WSS magnitude also reaches its peak. It is clearly observed that, there is an inverse relationship between the diameter of artery and WSS. The contour plot of turbulent

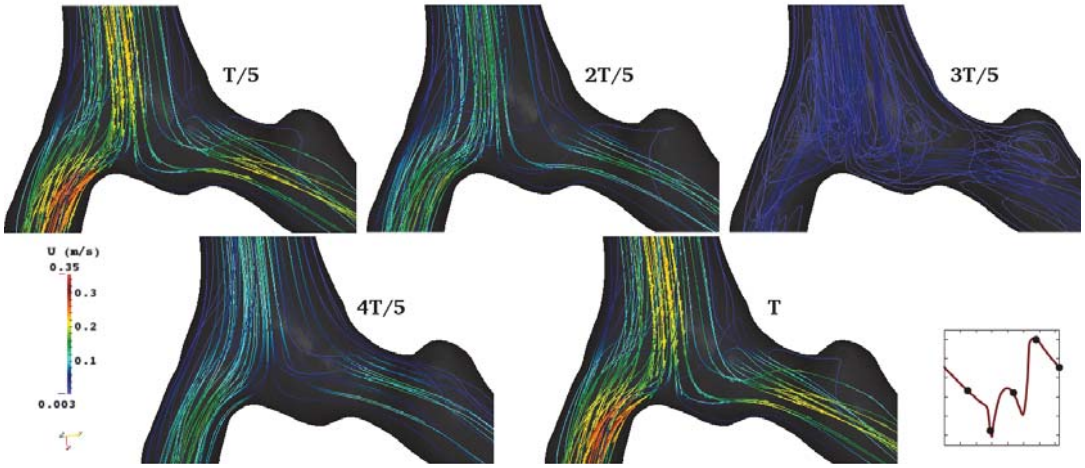

Fig. 4. Stream traces at the LCA first bifurcation coloured using the magnitude of instantaneous velocity.

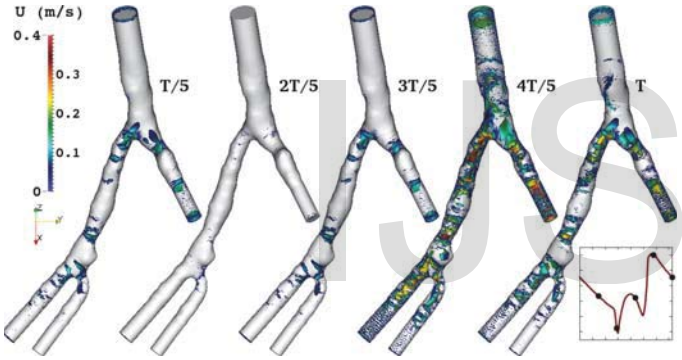

Fig. 6. Iso-surfaces drawn using the Q-criterion showing the Lagrangian coherent structures having a value of $(V_a/D)^2$ coloured using the instantaneous flow velocity, where V_a and D and average velocity and diameter of LCA respectively.

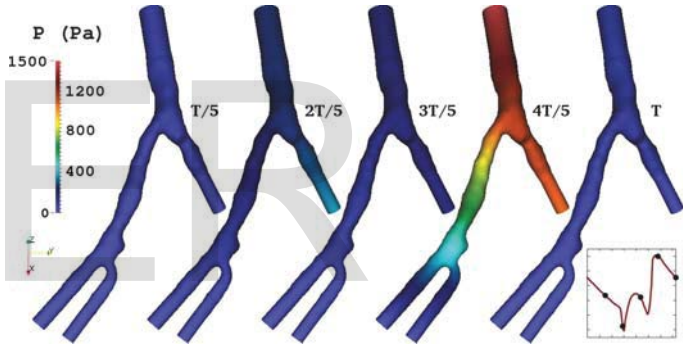

Fig. 7. Spacial distribution of pressure over the LCA surface during one time period of inlet pulse.

vortical structures shown in Fig. 6, drawn using the Q-criterion of Hunt et.al [21] reveals the presence of Lagrangian coherent structures which last for a significant amount of time in the flow field, around high WSS regions. The temporal pressure distribution given in Fig. 7 predicts a maximum gradient of around $1450\ Pa$ inside LCA. Fig. 8 shows the evolution of centreline velocity at different axial locations of the left coronary throughout the pulsatile cycle. Seven locations viz, proximal LCA (LCA-p), distal LCA (LCA-d), proximal LAD (LAD-p), distal LAD (LAD-d), distal D1 (D1-d), proximal LCX (LCX-p) and distal LCX(LCX-d) are monitored for velocity fluctuations with time . The profiles are presented for the whole simulation time of $10\ s$ and the enlarged view of final time period is given in the right.

IV. Conclusions and Future work

This study investigates patient specific flow patterns inside a human left coronary artery under normal physiological conditions. A framework using open source software is developed for the simulation of fluid mechanics of blood in coronary arteries using CFD techniques with geometries extracted from CT datasets. The open source toolkit VMTK and the meshing/solver package OpenFOAM are successfully applied to predict unsteady hemodynamics. The important conclusions are,

- Maximum values of WSS occurs at minimum diameter regions of the flow passage.
- WSS is found to be minimum at regions distributed around the bifurcations.
- Curvature of artery has a direct dependence on the minimum and peak values of WSS and the connection between radius, curvature and WSS is a subject to future studies.

V. Acknowledgments

The authors would like to thank the Center for Engineering Research and Development for the financial assistance.

References

[1] W. W. Nichols and M. F. O'Rourke, *McDonald's blood flow in arteries: theoretical, experimental, and clinical principles*. CRC Press, 2011.

[2] W. F. Boron and E. L. Boulpaep, *Medical Physiology, 2e Updated Edition*. Elsevier Health Sciences, 2012.

[3] D. N. Ku, "Blood flow in arteries," *Annual Review of Fluid Mechanics*, vol. 29, no. 1, pp. 399–434, 1997.

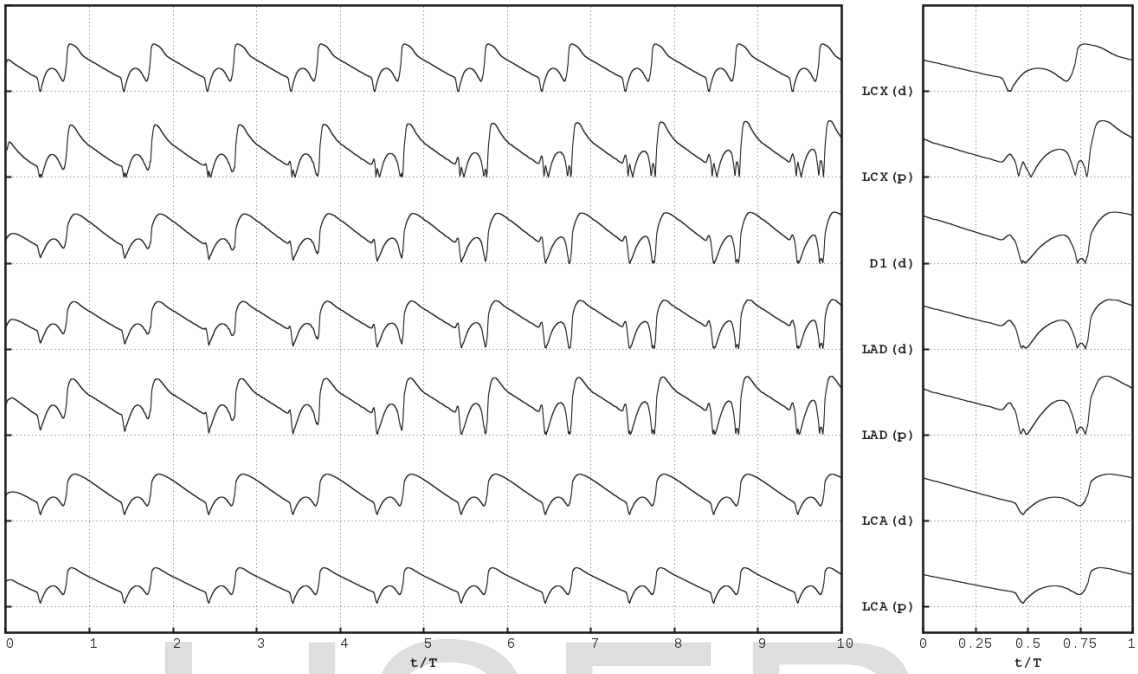

Fig. 8. Evolution of centreline velocity at different axial locations of the left coronary artery.

[4] G. Giannoglou, J. Soulis, T. Farmakis, D. Farmakis, and G. Louridas, "Haemodynamic factors and the important role of local low static pressure in coronary wall thickening," *International Journal of Cardiology*, vol. 86, no. 1, pp. 27 – 40, 2002.

[5] X. He and D. N. Ku, "Pulsatile flow in the human left coronary artery bifurcation: average conditions," *Journal of biomechanical engineering*, vol. 118, no. 1, pp. 74–82, 1996.

[6] C. A. Taylor and M. T. Draney, "Experimental and computational methods in cardiovascular fluid mechanics," *Annu. Rev. Fluid Mech.*, vol. 36, pp. 197–231, 2004.

[7] E. WF, H. RH, and B. J, "Coronary disease among United states soldiers killed in action in korea: Preliminary report," *Journal of the American Medical Association*, vol. 152, no. 12, pp. 1090–1093, 1953.

[8] P. Grøttum, A. Svindland, and L. Wallre, "Localization of atherosclerotic lesions in the bifurcation of the main left coronary artery," *Atherosclerosis*, vol. 47, no. 1, pp. 55 – 62, 1983.

[9] K. Perktold, M. Hofer, G. Rappitsch, M. Loew, B. Kuban, and M. Friedman, "Validated computation of physiologic flow in a realistic coronary artery branch," *Journal of Biomechanics*, vol. 31, no. 3, pp. 217 – 228, 1997.

[10] J. V. Soulis, T. M. Farmakis, G. D. Giannoglou, and G. E. Louridas, "Wall shear stress in normal left coronary artery tree," *Journal of Biomechanics*, vol. 39, no. 4, pp. 742 – 749, 2006.

[11] T. Chaichana, Z. Sun, and J. Jewkes, "Computation of hemodynamics in the left coronary artery with variable angulations," *Journal of Biomechanics*, vol. 44, no. 10, pp. 1869 – 1878, 2011.

[12] H. Samady, P. Eshtehardi, M. C. McDaniel, J. Suo, S. S. Dhawan, C. Maynard, L. H. Timmins, A. A. Quyyumi, and D. P. Giddens, "Coronary artery wall shear stress is associated with progression and transformation of atherosclerotic plaque and arterial remodeling in patients with coronary artery disease," *Circulation*, vol. 124, no. 7, pp. 779–788, 2011.

[13] OpenFOAM, "User's guide," *Version 2.1.1, www.openfoam.org*, 2013.

[14] M. Schaap, C. T. Metz, T. van Walsum, A. G. van der Giessen, A. C. Weustink, N. R. Mollet, C. Bauer, H. Bogunovi, C. Castro, X. Deng, E. Dikici, T. ODonnell, M. Frenay, O. Friman, M. H. Hoyos, P. H. Kitslaar, K. Krissian, C. Khnel, M. A. Luengo-Oroz, M. Orkisz, rjan Smedby, M. Styner, A. Szymczak, H. Tek, C. Wang, S. K. Warfield, S. Zambal, Y. Zhang, G. P. Krestin, and W. J. Niessen, "Standardized evaluation methodology and reference database for evaluating coronary artery centerline extraction algorithms," *Medical Image Analysis*, vol. 13, no. 5, pp. 701 – 714, 2009.

[15] L. Antiga, M. Piccinelli, L. Botti, B. Ene-Iordache, A. Remuzzi, and D. Steinman, "An image-based modeling framework for patient-specific computational hemodynamics," *Medical & Biological Engineering & Computing*, vol. 46, no. 11, pp. 1097–1112, 2008.

[16] P. J. Carreau, "Rheological equations from molecular network theories," *Transactions of The Society of Rheology (1957-1977)*, vol. 16, no. 1, pp. 99–127, 1972.

[17] B. M. Johnston, P. R. Johnston, S. Corney, and D. Kilpatrick, "Non-newtonian blood flow in human right coronary arteries: steady state simulations," *Journal of biomechanics*, vol. 37, no. 5, pp. 709–720, 2004.

[18] A. G. van der Giessen, H. C. Groen, P.-A. Doriot, P. J. de Feyter, A. F. van der Steen, F. N. van de Vosse, J. J. Wentzel, and F. J. Gijsen, "The influence of boundary conditions on wall shear stress distribution in patients specific coronary trees," *Journal of Biomechanics*, vol. 44, no. 6, pp. 1089 – 1095, 2011.

[19] S. B. Pope, *Turbulent flows*. Cambridge university press, 2000.

[20] A. Henderson, "Paraview guide," *A Parallel Visualization Application, Kitware Inc.*, 2007.

[21] J. C. Hunt, A. Wray, and P. Moin, "Eddies, streams, and convergence zones in turbulent flows," in *Studying Turbulence Using Numerical Simulation Databases, 2*, vol. 1, 1988, pp. 193–208.